Pressure tensor and heat flux vector for inhomogeneous nonequilibrium fluids under the influence of three-body forces

Junfang Zhang and B. D. Todd*
Centre for Molecular Simulation, Swinburne University of Technology, P.O. Box 218, Hawthorn Victoria 3122, Australia
(Received 11 September 2003; published 31 March 2004)

We present a derivation of the pressure tensor and heat flux vector for inhomogeneous fluids under the influence of three-body forces. The derivation is based on the method of planes formalism of Todd, Evans, and Daivis [Phys. Rev. E **52**, 1627 (1995); **51**, 4362 (1995)]. Our derivation is validated against nonequilibrium molecular dynamics simulations of a confined fluid acted upon by a two-body Barker-Fisher-Watts force coupled with the Axilrod-Teller three-body force. Our method of planes calculations agree perfectly with the equivalent mesoscopic route of integrating the momentum and energy continuity equations directly from the simulation data. Our calculations reveal that three-body forces have an important consequence for the isotropic pressure, but have negligible influence on the shear stress (hence viscosity) and heat flux vector (hence thermal conductivity) for a confined simple fluid.

DOI: 10.1103/PhysRevE.69.031111 PACS number(s): 05.60.Cd, 05.20.Jj, 05.10.−a, 66.20.+d

I. INTRODUCTION

Practical implementations of the theory and computational methods of statistical mechanics have never been more sought after, due mainly to rapid developments in nanoscience and their technological offshoots. These applications range from the transport of natural gas through zeolites through to the operation and dynamics of protein motors. While many of these applications are relevant to equilibrium situations, there is a growing interest in applying the principles of nonequilibrium statistical mechanics to molecular fluids under flow conditions. Simulations of shear-induced flow by homogeneous nonequilibrium molecular dynamics (NEMD) methods are now well established and routine, with particular technological relevance to lubrication and polymer processing [1–5]. Over the past decade interest has also grown in the application of inhomogeneous NEMD techniques to fluids confined at the nanoscale [6–10]. For nonequilibrium environments one is interested in not only the standard thermodynamic and structural information relevant to equilibrium fluids, but also their transport properties, namely the transport of mass, momentum and energy.

The first simulation of planar Couette flow by inhomogeneous NEMD methods (i.e., atomic fluid confined between atomistic walls moving at constant and opposite velocities with respect to each other), was performed by Liem *et al.* [11]. Their simulations showed that in the limit of large wall spacing, inhomogeneous and homogeneous NEMD methods were consistent with each other. A problem still remained in the formal application of nonequilibrium statistical mechanics to compute the stress tensor and heat flux vector. For homogeneous flows the standard Irving-Kirkwood procedure [12] is well suited, but for strongly inhomogeneous flows (e.g., fluids confined by structured walls on the nanoscale) it cannot be used. This was clearly demonstrated by Todd *et al.* [13,14] to be a consequence of the differential operator O_{ij} that results from an expansion of the difference of δ functions specifying atomic positions. For homogeneous fluids this operator is unity and poses no complication: the result is the standard Irving-Kirkwood formulas for the pressure tensor and heat flux vector. The operator is not unity for inhomogeneous fluids, and while it is possible to obtain exact expressions of the position-dependent momentum and energy fluxes by this route [15] it is an involved computation.

In Refs. [13], [14] it was demonstrated how a formulation of the Irving-Kirkwood procedure in reciprocal space could greatly simplify the calculation of momentum and energy fluxes. This formulation, known as the ''method of planes'' (MOP), is valid for systems with planar geometry and flow in one direction. While the original papers were devoted to formally deriving nonequilibrium statistical mechanical expressions for the pressure tensor and heat flux vector for pairwise additive potentials, it was later shown [16] how the method may be generalized to compute any other relevant property exactly, such as the position-dependent density, temperature and streaming velocity.

The method of planes formalism demonstrated that the Irving-Kirkwood gauge is a direct and natural consequence of solving for the microscopic momentum and energy fluxes via the hydrodynamic continuity equations formulated in reciprocal space. No heuristic assumptions were made about pressure being the ''force across unit area;'' rather it is a natural consequence of the formalism. Since these derivations were published there have been a number of studies that have used the methodology in practical simulations of equilibrium and nonequilibrium fluids, e.g., Refs. [17], [18], as well as more theoretical papers addressing the vagueness of the definition of the pressure tensor, e.g., Ref. [19]. The method has been used for confined alkanes [20], polymers [21], the computation of elastic constants in thin films [22], and has recently been formulated for flows in cylindrical geometry [23].

In this paper we extend the method of planes formalism one step further, by formally deriving expressions for the pressure tensor and heat flux vector for fluids under the influence of three-body forces. We test our theoretical expres-

*Email address: btodd@swin.edu.au

sions by applying them to simulations of a confined atomic fluid under the influence of gravity driven flow. The fluid interacts with itself and the walls by a combination of a two-body Barker-Fisher-Watts potential [24] and a three-body Axilrod-Teller potential [25]. Our MOP calculations for the pressure tensor and heat flux vector are validated against equivalent calculations involving direct integration of the momentum and energy continuity equations (the so-called IMC and IEC methods [13,14]) and are in excellent agreement. Our simulations demonstrate that the inclusion of three-body forces has a significant influence on the isotropic pressure, in agreement with previously reported results for homogeneous NEMD simulations of three-body fluids [26]. However, for simple fluids the transport of momentum and energy is largely dependent only on the two-body potential. This agrees with previously reported results that indicated the three-body potential only contributes about 3% of the total shear viscosity [27].

II. THEORY

In the derivations that follow we designate the two-body and three-body force contributions to the total interatomic force as $\mathbf{F}_i^{(2)}$ and $\mathbf{F}_i^{(3)}$, respectively. $\mathbf{F}_{ij}^{(3)}$ is defined here to be the contribution to the total three-body force on atom i due to atom j. If $\phi_{ij}^{(2)}=\phi^{(2)}(\mathbf{r}_i,\mathbf{r}_j)$ is the two-body potential and $\phi_{ijk}^{(3)}=\phi^{(3)}(\mathbf{r}_i,\mathbf{r}_j,\mathbf{r}_k)$ is the three-body potential, then

$$\mathbf{F}_i^{(2)} \equiv \sum_j \mathbf{F}_{ij}^{(2)} = -\sum_j \left(\frac{\partial \phi_{ij}^{(2)}}{\partial \mathbf{r}_i} \right), \tag{1}$$

$$\mathbf{F}_i^{(3)} \equiv \sum_{jk} (\mathbf{F}_{ij}^{(3)} + \mathbf{F}_{ik}^{(3)}) = -\left[\sum_{jk} \left\{ \left(\frac{\partial \phi_{ijk}^{(3)}}{\partial \mathbf{r}_{ij}} \right) + \left(\frac{\partial \phi_{ijk}^{(3)}}{\partial \mathbf{r}_{ik}} \right) \right\} \right] \quad (\mathbf{r}_{ij} \equiv \mathbf{r}_i - \mathbf{r}_j), \tag{2}$$

$$\mathbf{F}_{ij}^{(3)} \equiv -\frac{\partial \phi_{ijk}^{(3)}}{\partial \mathbf{r}_{ij}}. \tag{3}$$

The geometry of our system is planar and is shown schematically in Fig. 1. A three-dimensional fluid is confined between planar parallel walls separated by length L_y in the y direction. A constant field drives the system away from equilibrium and is directed in the x direction. Thus, all thermodynamic and transport properties are functions of only y.

A. Pressure tensor

The method of planes derivation of the pressure tensor follows closely the original derivation in Ref. [13]. Briefly, the method involves defining the microscopic expressions for the mass and momentum densities, then Fourier transforming and integrating over the x, z directions (as physical properties are assumed uniform in x, z). One also takes the Fourier transform of the momentum continuity equation, substitutes in the microscopic **k**-space momentum flux and solves for the **k**-space pressure tensor. Finally one performs the inverse Fourier transform to recover the **r**-space pressure tensor.

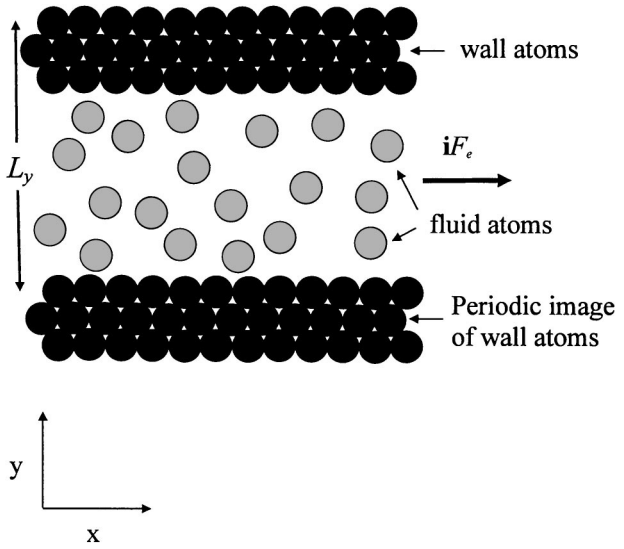

FIG. 1. Planar geometry of the flow for a confined fluid under the influence of an external field. The z axis is normal to the page.

In **k** space the spatially average momentum density is [13]

$$J_\alpha(k_y) = \frac{1}{A} \sum_i m v_{\alpha i} e^{i k_y y_i}, \tag{4}$$

where A is the area of the x-z surface that has its normal in the y direction. m and $v_{\alpha i}$ are the mass and laboratory velocity of particle i, respectively, and $\alpha = x, y, z$. Similarly, the **k**-space momentum continuity equation is

$$\frac{\partial J_\alpha(k_y)}{\partial t} = i k_y [P_{\alpha y}(k_y) + \mathcal{F}\{\rho(y) u_\alpha(y) u_y(y)\}], \tag{5}$$

where $\mathcal{F}\{\}$ denotes the Fourier transform of the quantity in brackets and **u** is the streaming velocity of the fluid. Substituting Eq. (4) into Eq. (5), isolating the pressure tensor, and finally inverse transforming gives the kinetic (K) and potential (U) contributions to the pressure tensor as

$$P_{\alpha y}^K(y) = \frac{1}{A} \sum_i \frac{p_{\alpha i} p_{y i}}{m} \delta(y_i - y) \tag{6}$$

and

$$P_{\alpha y}^U(y) = \frac{1}{2A} \sum_i F_{\alpha i} \, \mathrm{sgn}(y_i - y), \tag{7}$$

where $p_{\alpha i}$ and $p_{y i}$ are peculiar (i.e., thermal) momenta, and $F_{\alpha i}$ is the α component of the total force on atom i (i.e., it includes both two- and three-body contributions). The derivation up to this point is identical to the original derivation and the reader should refer to Ref. [13] for further details. It illustrates that Eqs. (6) and (7) are actually completely general for this type of planar symmetry and is valid for n-body forces. In what follows we specifically consider the case of three-body forces and use symmetry relations to generate a useful expression for the potential contribution to the three-body pressure. The kinetic contribution remains unchanged

as it implicitly contains the full two-plus three-body force contributions in the particle momenta.

We now separate out the two- and three-body contributions to the pressure

$$P^U_{\alpha y}(y) = \frac{1}{2A}\sum_i F_{\alpha i}\,\mathrm{sgn}(y_i - y)$$

$$= \frac{1}{2A}\sum_i (F^{(2)}_{\alpha i} + F^{(3)}_{\alpha i})\,\mathrm{sgn}(y_i - y)$$

$$= P^{(2)U}_{\alpha y}(y) + P^{(3)U}_{\alpha y}(y), \tag{8}$$

where $P^{(2)U}_{\alpha y}(y)$ and $P^{(3)U}_{\alpha y}(y)$ are contributions from two-body and three-body forces, respectively. In Ref. [13] it was shown that

$$P^{(2)U}_{\alpha y}(y) = \frac{1}{2A}\sum_i F^{(2)}_{\alpha i}\,\mathrm{sgn}(y_i - y)$$

$$= \frac{1}{4A}\left[\sum_{ij} F^{(2)}_{\alpha ij}\,\mathrm{sgn}(y_i - y) + \sum_{ij} F^{(2)}_{\alpha ji}\,\mathrm{sgn}(y_j - y)\right]$$

$$= \frac{1}{4A}\left\{\sum_{ij} F^{(2)}_{\alpha ij}[\mathrm{sgn}(y_i - y) - \mathrm{sgn}(y_j - y)]\right\}$$

$$= \frac{1}{2A}\sum_{ij} F^{(2)}_{\alpha ij}[\Theta(y_i - y)\Theta(y - y_j) - \Theta(y_j - y)\Theta(y - y_i)], \tag{9}$$

where Θ is the Heaviside step function.

Making similar use of particle exchange symmetry, the three-body contribution to the pressure tensor can be expressed as

$$P^{(3)U}_{\alpha y}(y) = \frac{1}{2A}\sum_i F^{(3)}_{\alpha i}\,\mathrm{sgn}(y_i - y)$$

$$= \frac{1}{6A}\left[\sum_i F^{(3)}_{\alpha i}\,\mathrm{sgn}(y_i - y) + \sum_j F^{(3)}_{\alpha j}\,\mathrm{sgn}(y_j - y) + \sum_k F^{(3)}_{\alpha k}\,\mathrm{sgn}(y_k - y)\right]. \tag{10}$$

Substitution of Eq. (2) into Eq. (10) yields

$$P^{(3)U}_{\alpha y}(y) = \frac{1}{6A}\left[\sum_{ij} F^{(3)}_{\alpha ij}\,\mathrm{sgn}(y_i - y) + \sum_{ik} F^{(3)}_{\alpha ik}\,\mathrm{sgn}(y_i - y) + \sum_{ji} F^{(3)}_{\alpha ji}\,\mathrm{sgn}(y_j - y) + \sum_{jk} F^{(3)}_{\alpha jk}\,\mathrm{sgn}(y_j - y) + \sum_{ki} F^{(3)}_{\alpha ki}\,\mathrm{sgn}(y_k - y) + \sum_{kj} F^{(3)}_{\alpha kj}\,\mathrm{sgn}(y_k - y)\right]$$

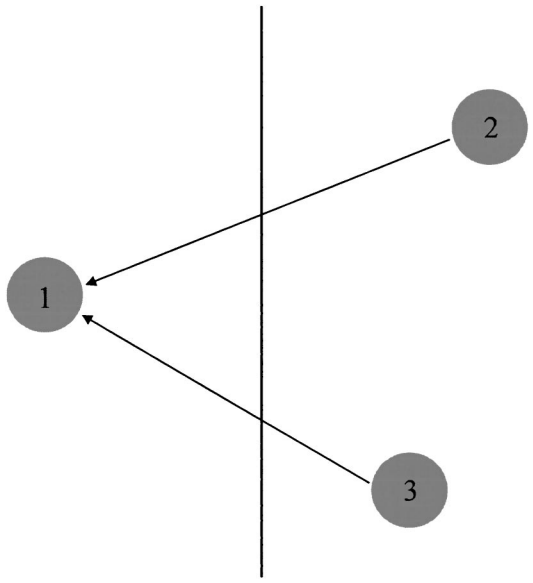

FIG. 2. Triangular configuration of atoms and the plane located at $y = y_0$. Contributions to the pressure tensor are included from atoms 1, 2, and 3 along the vectors $\mathbf{r}_{12}$ and $\mathbf{r}_{13}$.

$$= \frac{1}{6A}\left\{\sum_{ij} F^{(3)}_{\alpha ij}[\mathrm{sgn}(y_i - y) - \mathrm{sgn}(y_j - y)] + \sum_{ik} F^{(3)}_{\alpha ik}[\mathrm{sgn}(y_i - y) - \mathrm{sgn}(y_k - y)] + \sum_{jk} F^{(3)}_{\alpha jk}[\mathrm{sgn}(y_j - y) - \mathrm{sgn}(y_k - y)]\right\} \tag{11a}$$

$$= \frac{1}{3A}\left\{\sum_{ij} F^{(3)}_{\alpha ij}[\Theta(y_i - y)\Theta(y - y_j) - \Theta(y_j - y)\Theta(y - y_i)] + \sum_{ik} F^{(3)}_{\alpha ik}[\Theta(y_i - y)\Theta(y - y_k) - \Theta(y_k - y)\Theta(y - y_i)] + \sum_{jk} F^{(3)}_{\alpha jk}[\Theta(y_j - y)\Theta(y - y_k) - \Theta(y_k - y)\Theta(y - y_j)]\right\}. \tag{11b}$$

Equation (11) demonstrates that the potential contribution to the three-body pressure at a plane located at y occurs when components of the three-body force intersect that plane, in complete analogy with the two-body force contributions. For example, consider the situation shown in Fig. 2, in which a triangular configuration of three particles is shown. Only the force contributions along the vectors $\mathbf{r}_{12}$ and $\mathbf{r}_{13}$ intersect the plane at $y = y_0$ and contribute to the three-body pressure at this plane.

Finally, in a molecular dynamics simulation the full pressure tensor is computed by time averaging over the simulation phase space trajectory. In the case of the potential contributions this time averaging is straightforward. In Ref. [13]

it was shown that the time averaged kinetic component of the pressure tensor can be usefully expressed as

$$\langle P^K_{\alpha y}(y)\rangle = \lim_{t\to\infty}\frac{1}{At}\sum_{0<t_{i,m}<t}\sum_i p_{\alpha i}(t_{i,m})\mathrm{sgn}[p_{yi}(t_{i,m})]. \tag{12}$$

Here it is noted that particle i crosses the plane at y at a set of times $(t_{i,m}; i=1,...,N; m=1,2,...)$.

B. Heat flux vector

As with the pressure tensor derivation, we follow the method of planes formalism developed in Ref. [14] for the heat flux vector. That approach uses the microscopic definitions of the local energy density and the Fourier transform of the energy continuity equation to obtain a **k**-space expression for the heat flux vector, which is again back transformed into **r**-space.

We start the derivation at the Fourier transformed energy density continuity equation [14]

$$\frac{\partial}{\partial t}\rho e(\mathbf{k},t) = i\mathbf{k}\cdot[\mathbf{J}_q(\mathbf{k},t)+\mathcal{F}\{\rho e\mathbf{u}\}+\mathcal{F}\{\mathbf{P}\cdot\mathbf{u}\}]. \tag{13}$$

If $\mathbf{p}_i$ is defined here as the laboratory momentum of atom i, then the total energy of atom i is

$$e_i = \frac{\mathbf{p}_i^2}{2m}+\frac{1}{2}\sum_j \phi^{(2)}_{ij}+\frac{1}{3}\sum_{jk}\phi^{(3)}_{ijk}. \tag{14}$$

Noting that $\rho e\mathbf{u}(\mathbf{k},t)=\Sigma_i e_i\mathbf{u}(\mathbf{r}_i,t)e^{i\mathbf{k}\cdot\mathbf{r}_i}$ and $\rho e(\mathbf{k},t)=\Sigma_i e_i e^{i\mathbf{k}\cdot\mathbf{r}_i}$ [14], we first compute the time derivative of the energy density

$$\begin{aligned}\frac{\partial\rho e(\mathbf{k},t)}{\partial t} &= i\mathbf{k}\cdot\left(\sum_i \mathbf{v}_i e_i e^{i\mathbf{k}\cdot\mathbf{r}_i}\right)+\sum_i m\mathbf{v}_i\cdot\dot{\mathbf{v}}_i e^{i\mathbf{k}\cdot\mathbf{r}_i}+\frac{1}{2}\sum_{ij}\left(\dot{\mathbf{r}}_i\cdot\frac{\partial\phi^{(2)}_{ij}}{\partial\mathbf{r}_i}+\dot{\mathbf{r}}_j\cdot\frac{\partial\phi^{(2)}_{ij}}{\partial\mathbf{r}_j}\right)e^{i\mathbf{k}\cdot\mathbf{r}_i}+\frac{1}{3}\sum_{ijk}\left(\dot{\mathbf{r}}_i\cdot\frac{\partial\phi^{(3)}_{ijk}}{\partial\mathbf{r}_i}+\dot{\mathbf{r}}_j\cdot\frac{\partial\phi^{(3)}_{ijk}}{\partial\mathbf{r}_j}\right.\\
&\left.+\dot{\mathbf{r}}_k\cdot\frac{\partial\phi^{(3)}_{ijk}}{\partial\mathbf{r}_k}\right)e^{i\mathbf{k}\cdot\mathbf{r}_i} = i\mathbf{k}\cdot\left(\sum_i \mathbf{v}_i e_i e^{i\mathbf{k}\cdot\mathbf{r}_i}\right)+\sum_i \mathbf{v}_i\cdot(\mathbf{F}^{(2)}_i+\mathbf{F}^{(3)}_i)e^{i\mathbf{k}\cdot\mathbf{r}_i}-\frac{1}{2}\sum_{ij}(\mathbf{v}_i\cdot\mathbf{F}^{(2)}_{ij}+\mathbf{v}_j\cdot\mathbf{F}^{(2)}_{ji})e^{i\mathbf{k}\cdot\mathbf{r}_i}\\
&+\frac{1}{3}\sum_{ijk}\left(\dot{\mathbf{r}}_i\cdot\frac{\partial\phi^{(3)}_{ijk}}{\partial\mathbf{r}_i}+\dot{\mathbf{r}}_j\cdot\frac{\partial\phi^{(3)}_{ijk}}{\partial\mathbf{r}_j}+\dot{\mathbf{r}}_k\cdot\frac{\partial\phi^{(3)}_{ijk}}{\partial\mathbf{r}_k}\right)e^{i\mathbf{k}\cdot\mathbf{r}_i} = i\mathbf{k}\cdot\left(\sum_i \mathbf{v}_i e_i e^{i\mathbf{k}\cdot\mathbf{r}_i}\right)+\frac{1}{2}\sum_{ij}\mathbf{v}_i\cdot\mathbf{F}^{(2)}_{ij}(e^{i\mathbf{k}\cdot\mathbf{r}_i}-e^{i\mathbf{k}\cdot\mathbf{r}_j})\\
&+\sum_i \mathbf{v}_i\cdot\mathbf{F}^{(3)}_i e^{i\mathbf{k}\cdot\mathbf{r}_i}+\frac{1}{3}\sum_{ijk}\left(\dot{\mathbf{r}}_i\cdot\frac{\partial\phi^{(3)}_{ijk}}{\partial\mathbf{r}_i}+\dot{\mathbf{r}}_j\cdot\frac{\partial\phi^{(3)}_{ijk}}{\partial\mathbf{r}_j}+\dot{\mathbf{r}}_k\cdot\frac{\partial\phi^{(3)}_{ijk}}{\partial\mathbf{r}_k}\right)e^{i\mathbf{k}\cdot\mathbf{r}_i}.\end{aligned} \tag{15}$$

Consider now the two terms containing the three-body forces. The first term may be symmetrized as

$$\begin{aligned}\sum_i \mathbf{v}_i\cdot\mathbf{F}^{(3)}_i e^{i\mathbf{k}\cdot\mathbf{r}_i} &= \frac{1}{3}\left[\sum_i \mathbf{v}_i\cdot\mathbf{F}^{(3)}_i e^{i\mathbf{k}\cdot\mathbf{r}_i}+\sum_j \mathbf{v}_j\cdot\mathbf{F}^{(3)}_j e^{i\mathbf{k}\cdot\mathbf{r}_j}+\sum_k \mathbf{v}_k\cdot\mathbf{F}^{(3)}_k e^{i\mathbf{k}\cdot\mathbf{r}_k}\right]\\
&= \frac{1}{3}\left[\sum_{ijk}\mathbf{v}_i\cdot(\mathbf{F}^{(3)}_{ij}+\mathbf{F}^{(3)}_{ik})e^{i\mathbf{k}\cdot\mathbf{r}_i}+\sum_{ijk}\mathbf{v}_j\cdot(\mathbf{F}^{(3)}_{ji}+\mathbf{F}^{(3)}_{jk})e^{i\mathbf{k}\cdot\mathbf{r}_j}+\sum_{ijk}\mathbf{v}_k\cdot(\mathbf{F}^{(3)}_{ki}+\mathbf{F}^{(3)}_{kj})e^{i\mathbf{k}\cdot\mathbf{r}_k}\right].\end{aligned} \tag{16}$$

The second term containing three-body forces in Eq. (15) may be similarly expanded:

$$\begin{aligned}\frac{1}{3}\sum_{ijk}\left(\dot{\mathbf{r}}_i\cdot\frac{\partial\phi^{(3)}_{ijk}}{\partial\mathbf{r}_i}+\dot{\mathbf{r}}_j\cdot\frac{\partial\phi^{(3)}_{ijk}}{\partial\mathbf{r}_j}+\dot{\mathbf{r}}_k\cdot\frac{\partial\phi^{(3)}_{ijk}}{\partial\mathbf{r}_k}\right)e^{i\mathbf{k}\cdot\mathbf{r}_i} &= \frac{1}{3}\sum_{ijk}\left[\mathbf{v}_i\cdot\left(\frac{\partial\phi^{(3)}_{ijk}}{\partial\mathbf{r}_{ij}}+\frac{\partial\phi^{(3)}_{ijk}}{\partial\mathbf{r}_{ik}}\right)+\mathbf{v}_j\cdot\left(\frac{\partial\phi^{(3)}_{ijk}}{\partial\mathbf{r}_{ji}}+\frac{\partial\phi^{(3)}_{ijk}}{\partial\mathbf{r}_{jk}}\right)+\mathbf{v}_k\cdot\left(\frac{\partial\phi^{(3)}_{ijk}}{\partial\mathbf{r}_{ki}}\right.\right.\\
&\left.\left.+\frac{\partial\phi^{(3)}_{ijk}}{\partial\mathbf{r}_{kj}}\right)\right]e^{i\mathbf{k}\cdot\mathbf{r}_i}\\
&= -\frac{1}{3}\sum_{ijk}(\mathbf{v}_i\cdot\mathbf{F}^{(3)}_{ij}+\mathbf{v}_i\cdot\mathbf{F}^{(3)}_{ik}-\mathbf{v}_j\cdot\mathbf{F}^{(3)}_{ij}+\mathbf{v}_j\cdot\mathbf{F}^{(3)}_{jk}-\mathbf{v}_k\cdot\mathbf{F}^{(3)}_{ik}-\mathbf{v}_k\cdot\mathbf{F}^{(3)}_{jk})e^{i\mathbf{k}\cdot\mathbf{r}_i}.\end{aligned} \tag{17}$$

Defining $S^{(3)}$ as the sum of Eqs. (16) and (17) gives

$$S^{(3)} = \frac{1}{3}\sum_{ijk}[\mathbf{v}_j\cdot\mathbf{F}^{(3)}_{ij}(e^{i\mathbf{k}\cdot\mathbf{r}_i}-e^{i\mathbf{k}\cdot\mathbf{r}_j})-\mathbf{v}_j\cdot\mathbf{F}^{(3)}_{jk}(e^{i\mathbf{k}\cdot\mathbf{r}_i}-e^{i\mathbf{k}\cdot\mathbf{r}_j})+\mathbf{v}_k\cdot\mathbf{F}^{(3)}_{ik}(e^{i\mathbf{k}\cdot\mathbf{r}_i}-e^{i\mathbf{k}\cdot\mathbf{r}_k})+\mathbf{v}_k\cdot\mathbf{F}^{(3)}_{jk}(e^{i\mathbf{k}\cdot\mathbf{r}_i}-e^{i\mathbf{k}\cdot\mathbf{r}_k})]. \tag{18}$$

We now permute the triplet indices in Eq. (18) such that all velocities are in terms of the index i to obtain

$$S^{(3)}=\frac{1}{3}\sum_{ijk}\mathbf{v}_i\cdot[\mathbf{F}_{ik}^{(3)}+\mathbf{F}_{ij}^{(3)}](e^{i\mathbf{k}\cdot\mathbf{r}_i}-e^{i\mathbf{k}\cdot\mathbf{r}_k})+\frac{1}{3}\sum_{ijk}\mathbf{v}_i\cdot[\mathbf{F}_{ij}^{(3)}+\mathbf{F}_{ik}^{(3)}](e^{i\mathbf{k}\cdot\mathbf{r}_i}-e^{i\mathbf{k}\cdot\mathbf{r}_j})=\frac{1}{3}\sum_{ik}\mathbf{v}_i\cdot\mathbf{F}_i^{(3)}(e^{i\mathbf{k}\cdot\mathbf{r}_i}-e^{i\mathbf{k}\cdot\mathbf{r}_k})+\frac{1}{3}\sum_{ij}\mathbf{v}_i\cdot\mathbf{F}_i^{(3)}(e^{i\mathbf{k}\cdot\mathbf{r}_i}-e^{i\mathbf{k}\cdot\mathbf{r}_j}) \tag{19}$$

Substituting Eq. (19) back into Eq. (15) gives

$$\frac{\partial\rho e(\mathbf{k},t)}{\partial t}=i\mathbf{k}\cdot\left(\sum_i\mathbf{v}_ie_ie^{i\mathbf{k}\cdot\mathbf{r}_i}\right)+\frac{1}{2}\sum_{ij}\mathbf{v}_i\cdot\mathbf{F}_{ij}^{(2)}(e^{i\mathbf{k}\cdot\mathbf{r}_i}-e^{i\mathbf{k}\cdot\mathbf{r}_j})+\frac{1}{3}\sum_{ik}\mathbf{v}_i\cdot\mathbf{F}_i^{(3)}(e^{i\mathbf{k}\cdot\mathbf{r}_i}-e^{i\mathbf{k}\cdot\mathbf{r}_k})+\frac{1}{3}\sum_{ij}\mathbf{v}_i\cdot\mathbf{F}_i^{(3)}(e^{i\mathbf{k}\cdot\mathbf{r}_i}-e^{i\mathbf{k}\cdot\mathbf{r}_j}). \tag{20}$$

Substitution of Eq. (20) into the Fourier transformed energy continuity equation [i.e., Eq. (13)] yields

$$i\mathbf{k}\cdot\mathbf{J}_q(\mathbf{k},t)=i\mathbf{k}\cdot\left(\sum_i[\mathbf{v}_i-\mathbf{u}(\mathbf{r}_i,t)]e_ie^{i\mathbf{k}\cdot\mathbf{r}_i}\right)+\frac{1}{2}\sum_{ij}\mathbf{v}_i\cdot\mathbf{F}_{ij}^{(2)}(e^{i\mathbf{k}\cdot\mathbf{r}_i}-e^{i\mathbf{k}\cdot\mathbf{r}_j})+\frac{1}{3}\sum_{ij}\mathbf{v}_i\cdot\mathbf{F}_i^{(3)}(e^{i\mathbf{k}\cdot\mathbf{r}_i}-e^{i\mathbf{k}\cdot\mathbf{r}_j})+\frac{1}{3}\sum_{ik}\mathbf{v}_i\cdot\mathbf{F}_i^{(3)}(e^{i\mathbf{k}\cdot\mathbf{r}_i}-e^{i\mathbf{k}\cdot\mathbf{r}_k})-i\mathbf{k}\cdot\mathcal{F}\{\mathbf{P}\cdot\mathbf{u}\}. \tag{21}$$

Integrating over x and z, dividing by ik_y and taking the inverse Fourier transform yields

$$AJ_{qy}(y,t)=\sum_i(v_{yi}-u_y)e_i\delta(y-y_i)-\frac{1}{4}\sum_{ij}\mathbf{v}_i\cdot\mathbf{F}_{ij}^{(2)}[\mathrm{sgn}(y-y_i)-\mathrm{sgn}(y-y_j)]-\frac{1}{6}\sum_{ij}\mathbf{v}_i\cdot\mathbf{F}_i^{(3)}[\mathrm{sgn}(y-y_i)-\mathrm{sgn}(y-y_j)]-\frac{1}{6}\sum_{ik}\mathbf{v}_i\cdot\mathbf{F}_i^{(3)}[\mathrm{sgn}(y-y_i)-\mathrm{sgn}(y-y_k)]-A\{\mathbf{P}\cdot\mathbf{u}\}_y. \tag{22}$$

To complete the derivation, we substitute the MOP expression for the pressure tensor, Eq. (11a), into Eq. (22) to give the kinetic and potential contributions to the heat flux vector

$$J_{qy}(y,t)=J_{qy}^K(y,t)+J_{qy}^U(y,t). \tag{23}$$

The kinetic contribution is, as with the pressure tensor, identical in form to the original MOP derivation in Ref. [14]:

$$J_{qy}^K(y,t)=\frac{1}{A}\sum_i[v_{yi}-u(y)]U_i\delta(y-y_i) \tag{24}$$

except that here U_i is the internal energy of a particle defined as

$$U_i=\frac{1}{2}m[\mathbf{v}_i-\mathbf{u}(y_i)]^2+\frac{1}{2}\sum_j\phi_{ij}^{(2)}+\frac{1}{3}\sum_{jk}\phi_{ijk}^{(3)}. \tag{25}$$

The potential contribution to the heat flux vector is

$$J_{qy}^U(y,t)=-\frac{1}{4A}\sum_{ij}[\mathbf{v}_i-\mathbf{u}(y)]\cdot\mathbf{F}_{ij}^{(2)}[\mathrm{sgn}(y-y_i)-\mathrm{sgn}(y-y_j)]-\frac{1}{6A}\sum_{ij}[\mathbf{v}_i-\mathbf{u}(y)]\cdot\mathbf{F}_{ij}^{(3)}\times[\mathrm{sgn}(y-y_i)-\mathrm{sgn}(y-y_j)]-\frac{1}{6A}\sum_{ik}[\mathbf{v}_i-\mathbf{u}(y)]\cdot\mathbf{F}_{ik}^{(3)}\times[\mathrm{sgn}(y-y_i)-\mathrm{sgn}(y-y_k)]-\frac{1}{6A}\sum_{ijk}\mathbf{v}_i\cdot\mathbf{F}_{ij}^{(3)}\times[\mathrm{sgn}(y-y_i)-\mathrm{sgn}(y-y_k)]-\frac{1}{6A}\sum_{ijk}\mathbf{v}_i\cdot\mathbf{F}_{ik}^{(3)}\times[\mathrm{sgn}(y-y_i)-\mathrm{sgn}(y-y_j)]+\frac{1}{6A}\sum_{jk}\mathbf{u}(y)\cdot\mathbf{F}_{jk}^{(3)}\times[\mathrm{sgn}(y-y_j)-\mathrm{sgn}(y-y_k)]. \tag{26}$$

An alternative, more concise form of Eq. (26), may be derived by substituting the unsymmetrised form of the pressure tensor [i.e., Eq. (8)] into Eq. (22). This is demonstrated in the Appendix and the result is quoted here as

$$J_{qy}^U(y,t)=-\frac{1}{2A}\sum_i[\mathbf{v}_i-\mathbf{u}(y)]\cdot\mathbf{F}_i^{(2)}\,\mathrm{sgn}(y-y_i)-\frac{1}{2A}\sum_i[\mathbf{v}_i-\mathbf{u}(y)]\cdot\mathbf{F}_i^{(3)}\,\mathrm{sgn}(y-y_i)+\frac{1}{6A}\sum_{ijk}\mathbf{v}_i\cdot\mathbf{F}_i^{(3)}[\mathrm{sgn}(y-y_i)+\mathrm{sgn}(y-y_j)+\mathrm{sgn}(y-y_k)]. \tag{27}$$

The last three terms in Eq. (26) and the last term in Eq. (27) are not direct analogies of the two-body heat flux, unlike the case in the pressure tensor three-body expressions, which are direct analogies. They are a result of particle velocities coupling to three-body forces, which does not occur in the pressure tensor calculation. However, it will be shown in

Sec. IV that these additional terms are negligible, if not zero. As was the case for the kinetic term for the pressure tensor, the kinetic term for the heat flux vector in Eq. (24) can be written in a more useful way for computer simulation as [14]

$$J_{qy}^{K}(y)=\lim_{t\to\infty}\frac{1}{At}\sum_{0<t_{i,m}<t}U_i\,\mathrm{sgn}[c_{yi}(t_{i,m})], \tag{28}$$

where $\mathbf{c}_i\equiv\mathbf{v}_i-\mathbf{u}(y)$ is the plane peculiar velocity of atom i.

III. SIMULATIONS

A. Two- and three-body potentials

Our simulations are performed on fluid and solid atoms that interact via the Barker-Fisher-Watts two-body potential [24] and Axilrod-Teller three-body potential [25]. The total intermolecular potential (ϕ) is a contribution from two-body interactions ($\phi^{(2)}$) and three-body dispersion interactions ($\phi^{(3)}$):

$$\phi(r)=\phi^{(2)}(r)+\phi^{(3)}(r). \tag{29}$$

The two-body interaction of argon is well represented by the Barker-Fisher-Watts (BFW) potential [24]. The BFW potential is a linear combination of the Barker-Pompe [28] (ϕ_{BP}) and Bobetic-Barker [29] (ϕ_{BB}) potentials

$$\phi^{(2)}(r)=0.75\phi_{\mathrm{BB}}(r)+0.25\phi_{\mathrm{BP}}(r), \tag{30}$$

where the potentials of Barker-Pompe and Bobetic-Barker have the following form:

$$\phi^{(2)}(r)=\varepsilon\left[\sum_{i=0}^{5}A_i(x-1)^i\exp[\alpha(1-x)]-\sum_{j=0}^{2}\frac{C_{2j+6}}{\delta+x^{2j+6}}\right]. \tag{31}$$

Here, $x=r/r_m$ where r_m is the intermolecular separation at which the potential has a minimum value and the other parameters are listed in Table I.

The triple-dipole Axilrod-Teller (AT) potential [25] is

$$\phi^{(3)}(\mathbf{r}_i,\mathbf{r}_j,\mathbf{r}_k)=\frac{v_{DDD}(1+3\cos\theta_i\cos\theta_j\cos\theta_k)}{(r_{ij}r_{ik}r_{jk})^3}, \tag{32}$$

where v_{DDD} is the nonadditive coefficient, and the angles and intermolecular separations refer to a triangular configuration of atoms. The nonadditive coefficient for argon is 518.3 a.u. [30]. Recent work [31] has demonstrated that the Axilrod-Teller term can significantly improve the prediction of liquid phase properties.

TABLE I. Parameters for the Barker-Fisher-Watts potential.

	Argon	
$\varepsilon/k(K)$	142.095	
$\sigma(A)$	3.3605	
$r_m(A)$	3.7612	
	Barker-Pompe	Bobetic-Barker
$\varepsilon/k(K)$	147.70	140.235
$r_m(A)$	3.7560	3.7630
$\sigma(A)$	3.341	3.3666
A_0	0.2349	0.29214
A_1	−4.7735	−4.41458
A_2	−10.2194	−7.70182
A_3	−5.2905	−31.9293
A_4	0.0	−136.026
A_5	0.0	−151.00
C_6	1.0698	1.11976
C_8	0.1642	0.171551
C_{10}	0.0132	0.013748
α	12.5	12.5
δ	0.01	0.01

B. Geometry and equations of motion

The geometry of our simulation cell is shown in Fig. 1. An atomic fluid is confined between atomistic walls as depicted. Our geometry is such that $y=0$ defines the center of the fluid channel. A field (e.g., gravity) representing a constant pressure head drives the fluid and is directed in the x direction. Each wall is three atomic layers thick, and the second wall is just the periodic image of the first. The entire cell is thus periodic in x, y, and z. The total number of atoms is $N=324$, which includes 270 liquid atoms and 54 wall atoms ($N_w=18$ atoms per layer). In what follows all quantities are expressed in reduced units. The density of the fluid is 0.44 and the wall density is 0.84. The cell dimensions are $L_x=5.0565$, $L_y=27.5143$, $L_z=5.0565$. The thickness of the walls is $\Delta y_w=2.5143$. We use the same method in Ref. [13] to approximate the accessible width of the fluid channel, which gives an effective pore width of $l_y=24.0871$. A cutoff potential radius of $L_x/2=2.5282$ was used for the two-body force calculation, whereas a value of $L_x/4=1.2641$ was used for the three-body force. These were optimal values, based upon the work performed in Ref. [31]. In our simulations we used a truncated and shifted version of the BFW and AT potentials, so that long-range corrections need not be considered. In this way the potential is zero at and beyond the cutoff value. We justify this as our goal is to verify the MOP expressions derived in Sec. II for the pressure tensor and heat flux vector, rather than to accurately reproduce experimental results.

The equations of motion used to simulate wall and fluid atoms were developed in Ref. [13] and quoted here as follows, modified for three-body forces. We note that wall atoms interact via the two plus three body forces in addition to a harmonic spring force that tethers them together. For the wall particles,

$$\dot{\mathbf{r}}_i=\frac{\mathbf{p}_i}{m}$$

$$\dot{\mathbf{p}}_i=-K(\mathbf{r}_i-\mathbf{q}_i)+\mathbf{F}_i^{(2)}+\mathbf{F}_i^{(3)}-\alpha\mathbf{p}_i-\mathbf{j}\lambda_{L_n},\quad i\in L_n. \tag{33}$$

K is the spring force constant and was set to 57.15 in all simulations. $\mathbf{q}_i$ is the equilibrium ''frozen'' lattice position of

atom i. $\mathbf{r}_i$ is the laboratory position of atom i and $\mathbf{p}_i$ here refers to the laboratory momentum of atom i. As the walls are not under the influence of a gravitational force the streaming velocity is zero and the peculiar (thermal) and laboratory momenta are equivalent. $\mathbf{j}$ is the unit vector in the y direction and the layer multiplier λ_{L_n} ensures that the center of mass of each wall layer stays fixed, where the index $n=1$, 2, 3, refers to the wall layer. This is important otherwise the walls separate as the fluid heats up under flow. α is a thermostat multiplier used to keep the temperature of the walls fixed (in our simulations the wall temperature was fixed at 0.722). The layer multiplier and thermostat are computed as

$$\lambda_{L_n}=\frac{\mathbf{j}}{N_w}\sum_{i\in L_n}^{N_w}[-K(\mathbf{r}_i-\mathbf{q}_i)+\mathbf{F}_i^{(2)}+\mathbf{F}_i^{(3)}], \tag{34}$$

where

$$\sum_{L_n=1}^{3}\sum_{i\in L_n}^{N_w}1=3N_w$$

and

$$\alpha=\frac{\Sigma_{i\in L}^{3N_w}\{[-K(\mathbf{r}_i-\mathbf{q}_i)+\mathbf{F}_i^{(2)}+\mathbf{F}_i^{(3)}-\mathbf{j}\lambda_{L_n}]\cdot\mathbf{p}_i\}}{\Sigma_{i\in L}^{3N_w}\mathbf{p}_i^2}. \tag{35}$$

Here $L=\{L_1,L_2,L_3\}$.

The fluid atoms obey Newton's equations of motion

$$\dot{\mathbf{r}}_i=\frac{\mathbf{p}_i}{m}$$

$$\dot{\mathbf{p}}_i=\mathbf{F}_i^{(2)}+\mathbf{F}_i^{(3)}+\mathbf{i}F_e, \tag{36}$$

where F_e is the external driving field and $\mathbf{i}$ is the unit vector in the x direction and we again note that $\mathbf{r}_i$ and $\mathbf{p}_i$ refer to the laboratory position and momentum of atom i, respectively. In our simulations the field strength used was $F_e=0.2$.

The equations of motion were solved with a fifth order Gear predictor-corrector scheme with an integration time step of $\tau=0.001$. Our simulations were first run for a total of 10^6 time steps to reach a nonequilibrium steady state. Once steady state was achieved, production runs of a total of 10^7 time steps were run with averages accumulated in blocks of 50 000 time steps. The errors presented in our plots represent the standard error in the mean.

In our simulations we do not assume any functional form for the streaming velocity. Rather, we first run a steady-state simulation of $\sim 10^6$ time steps and compute a time-averaged velocity profile at planes, using the procedure developed in Ref. [16]. These plane velocity values are then used as the streaming velocity $u_x(y)$ in MOP calculations of the pressure tensor and heat flux vector in all subsequent production runs.

Finally, we note that a total of 200 planes were used in the MOP calculations, though not all planes data are plotted on the figures presented in this work for clarity of visualization. For further details of the simulation methodology, readers are referred to Refs. [13], [14], [16].

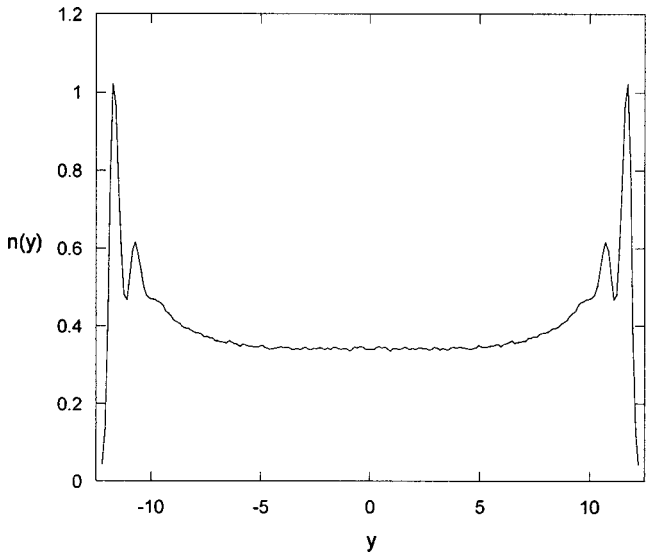

FIG. 3. Number density profile for the fluid system.

IV. RESULTS AND DISCUSSION

In Figs. 3 and 4 we plot the density and streaming velocity profiles, respectively. The streaming velocity is seen to be well represented by a symmetric quadratic function in y, in conformity with hydrodynamics [13]. Only near the walls does the streaming velocity deviate from quadratic behavior. It is well known that hydrodynamics breaks down at smaller channel widths [32].

In Fig. 5 we plot MOP calculations of P_{yy}, the y component of the pressure in the direction normal to the wall surface, for both the BFW fluid and the BFW fluid with the inclusion of the AT three body forces. For mechanical stability P_{yy} must be constant throughout the channel, and this is indeed seen to be the case. Also shown is the pressure cal-

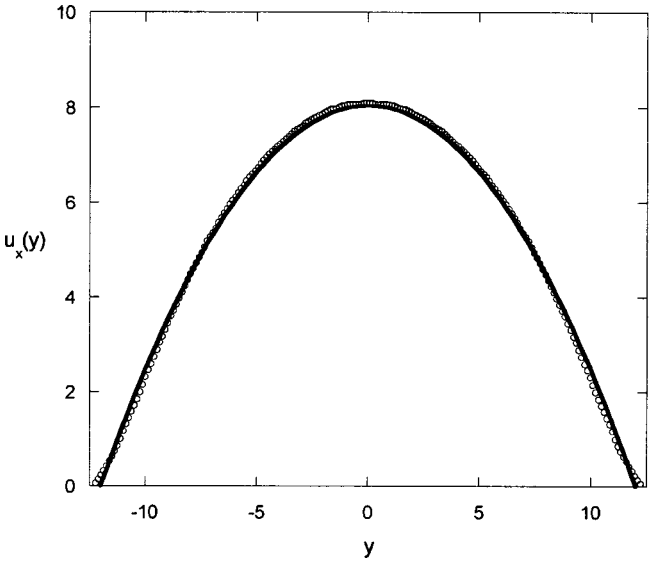

FIG. 4. Streaming velocity profile (circle data points) for the fluid. Superimposed (solid curve) is a symmetric quadratic fit, in conformity with hydrodynamic prediction. Error bars are the size of the plotting symbol.

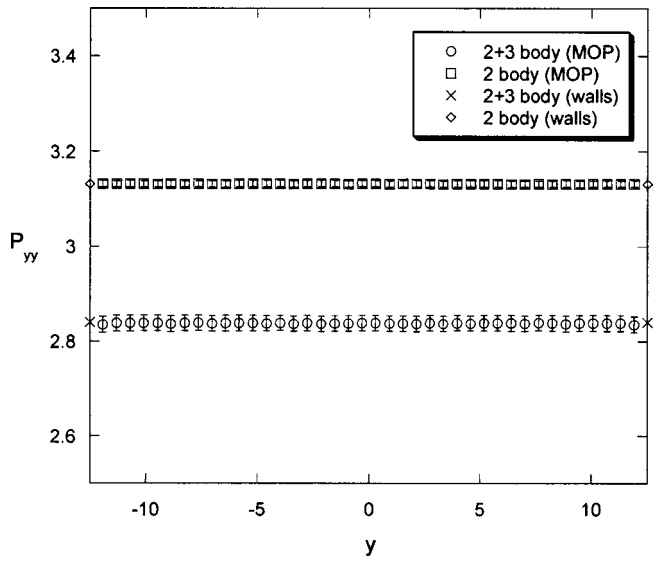

FIG. 5. P_{yy} as a function of y for the BFW and BFW+AT fluids. The pressure is computed by the method of planes. Also shown is the pressure at the walls.

culated on the system walls. This is computed from the total y component of the force per unit area exerted on the wall atoms by fluid atoms on one side of the wall. We see perfect agreement between wall and fluid P_{yy} values, as expected. Clearly the addition of the three-body force significantly affects the pressure P_{yy}. Neglecting to include three-body forces overestimates the pressure by almost 11%.

Of greater interest to us is the shear stress $(-P_{xy})$. In Fig. 6(a) we plot P_{xy} as a function of y for the BFW and BFW +AT fluids. We show the results of our MOP calculations and compare them with direct integration of the momentum continuity equation (the IMC method of Ref. [13], given as $P_{xy}(y)=F_e\int_0^y dy' n(y')$, where $n(y)$ is the number density). Error bars are of the order of the size of the plotting symbols. We find excellent agreement between both methods, demonstrating that the MOP calculations are correct. The value of P_{xy} calculated at the walls is also included and seen to be consistent with both the MOP and IMC values. Note that the stress deviates from the linear hydrodynamics prediction close to the walls, as is to be expected for such an inhomogeneous system. From Fig. 6(a) it is clear that three-body forces have negligible effect on the shear stress. This is seen more clearly in Fig. 6(b), in which the region between $5.7 \leqslant y \leqslant 6.1$ is magnified. This is consistent with the observations reported in Ref. [27] that showed that three-body forces only affected the shear viscosity by approximately 3%. The precise degree of influence is likely to depend on temperature and density, and to a lesser degree the number of atoms, so we do not say anything conclusive at this stage. We also note that our potentials are shifted and truncated and include no long-range corrections.

In Fig. 7(a) we plot the heat flux vector as a function of y for the BFW and BFW+AT fluids. Classical hydrodynamics predicts a cubic heat flux profile. We again show the results of our MOP calculations and compare them with direct integration of the energy continuity equation [the IEC method of

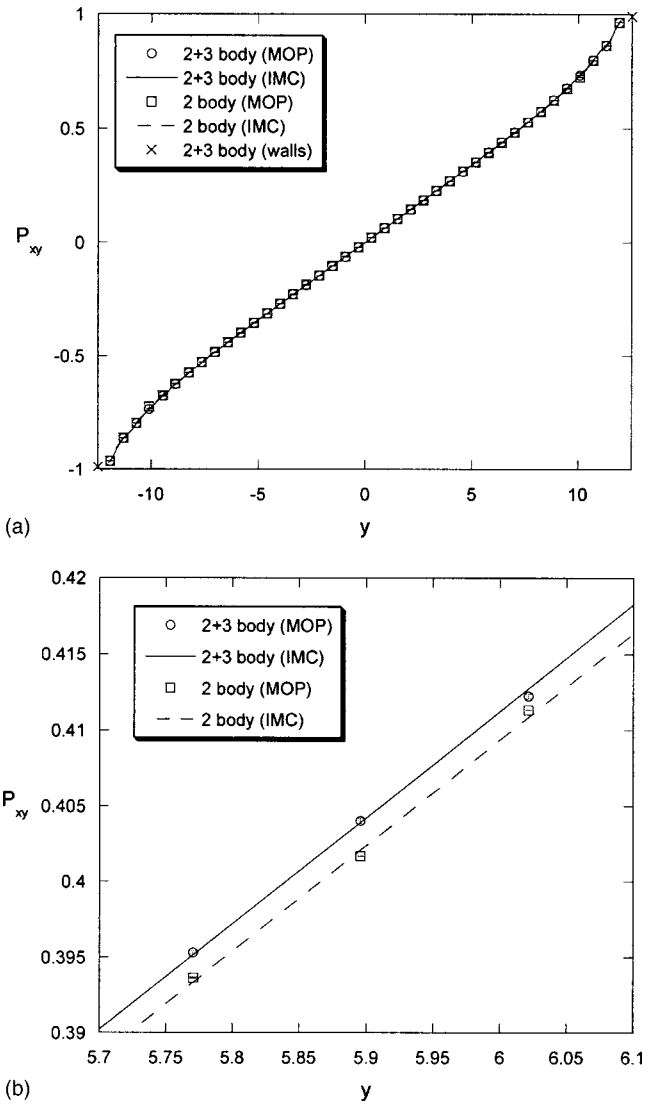

FIG. 6. (a) P_{xy} as a function of y for the BFW and BFW+AT fluids. P_{xy} computed by the MOP and IMC methods are shown, as well as P_{xy} computed at the walls. (b) As with (a) but magnified in the range $5.7 \leqslant y \leqslant 6.1$.

Ref. [14] given as $J_{qy}(y)=-\int_0^y dy' P_{xy}(y')\dot{\gamma}(y')$, where $\dot{\gamma}$ is the strain rate, $\dot{\gamma}=\partial u_x(y)/\partial y]$. Error bars are of the order of plotting symbol sizes. Once again, excellent agreement is found between both methods, confirming the validity of the MOP expressions. For a channel this size it is clear that the classical cubic heat flux profile is obeyed. The value of the heat flux at the walls was also computed by noting that the Gaussian thermostat acting on the walls removes heat at a rate of

$$\dot{Q}(t)=\alpha(t)\sum_{i=1}^{N}\frac{\mathbf{p}_i^2}{m}. \tag{37}$$

The heat flux at the walls is therefore

$$\langle J_{qy}(y=y_{wall})\rangle=\frac{1}{A}\langle K_w\alpha\rangle, \tag{38}$$

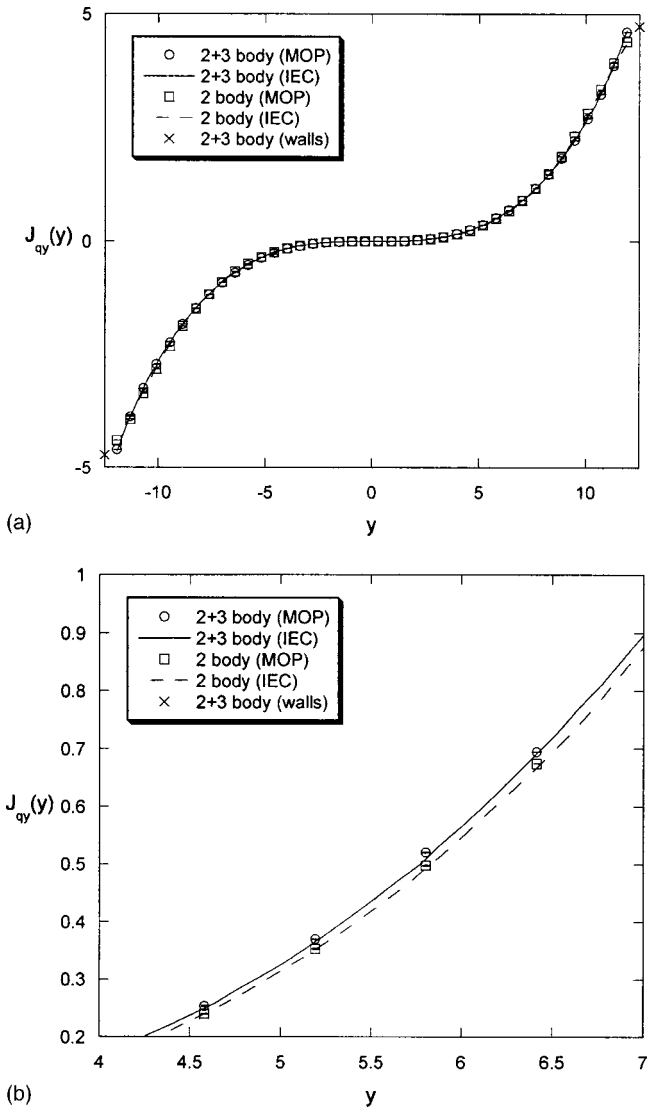

FIG. 7. (a) Heat flux vector $J_{qy}(y)$ as a function of y for the BFW and BFW+AT fluids. $J_{qy}(y)$ computed by the MOP and IEC methods are shown, as well as $J_{qy}(y)$ computed at the walls. (b) As with (a) but magnified in the range $4.0 \leqslant y \leqslant 7.0$.

where K_w is the kinetic energy of the wall atoms and the angle brackets indicate a time average [14]. The heat flux at the walls is in excellent agreement with the MOP and IEC values at the wall-fluid interface.

We again observe that the presence of three-body forces has very little influence in the transportation of energy across the channel. In Fig. 7(b) the region between $4.0 \leqslant y \leqslant 7.0$ is magnified. Three-body forces contribute a very small but noticeable effect on the heat flux, slightly increasing its magnitude. Again, this effect is likely to be temperature and density dependent and we refrain from specific conclusions at this stage. What is import for our purposes is the excellent agreement between the MOP and IEC methods, clearly visible in this figure.

Finally, in Fig. 8 we plot several contributions to the three-body component of the heat flux vector. Term 1 (circles) represents the second and third terms in Eq. (26). These terms are the direct three-body analogy of the two-body contribution to the heat flux vector. Term 2 (diamonds) represents the additional last three terms in Eq. (26). It is clear that these last three terms are negligible, if not zero.

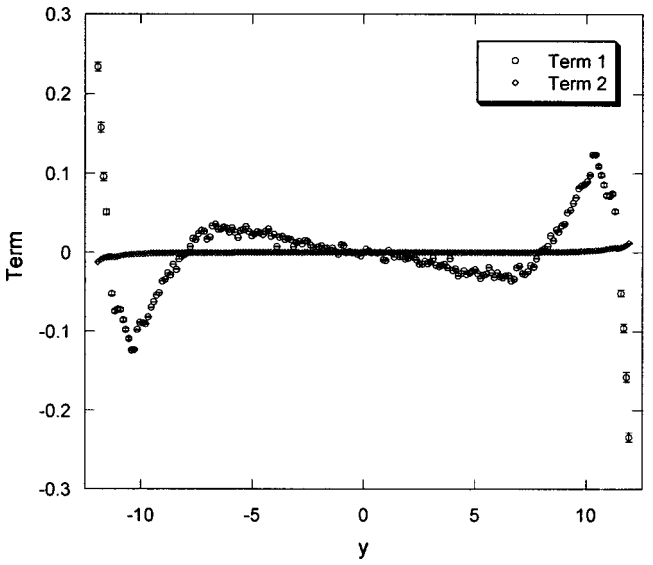

FIG. 8. Individual terms of the three-body contribution to the heat flux vector. Term 1 represents the second and third terms of Eq. (26) and is the direct analogy of the two-body contribution to the heat flux vector. Term 2 represents the last three terms in Eq. (26).

V. CONCLUSIONS

In this paper we have derived method of planes expressions for the pressure tensor and heat flux vector for a fluid under the influence of three-body forces. Our derivations have been validated against numerical simulations of gravity driven flow by nonequilibrium molecular dynamics methods. The MOP calculations are in excellent agreement with independent calculations based upon direct integration of the hydrodynamic momentum and energy continuity equations. Our results show that the isotropic pressure is sensitive to the presence of three-body forces, whereas the shear stress and heat flux vector seem to be largely independent of them. Further work is required to study the temperature and density dependence on the relative magnitudes of the two to three-body force contributions. While such effects are clearly small for noble gas fluids such as argon, they will most likely play a significant and important role for heavier atomic and molecular fluids and liquid metals. It is hoped that our MOP expressions will be useful for the study of such liquids in the future.

ACKNOWLEDGMENTS

J.Z. acknowledges the Australian government for financial assistance. Computations were performed on the supercomputing facilities at the Australian Partnership for Advanced Computing (APAC), through a generous grant of computer time.

APPENDIX

An alternative form of Eq. (26) may be obtained by using the alternative (unsymmetrised) form of the pressure tensor in Eq. (8), i.e.,

$$P_{\alpha y}^{U(3)}(y,t) = -\frac{1}{2A}\sum_i F_{\alpha i}^{(3)} \operatorname{sgn}(y-y_i). \tag{A1}$$

Substituting Eq. (A1) into Eq. (22) gives

$$\begin{aligned} AJ_{qy}(y,t) = &\sum_i (v_{yi}-u_y)e_i\delta(y-y_i) - \frac{1}{4}\sum_{ij} \mathbf{v}_i\cdot\mathbf{F}_{ij}^{(2)} \\ &\times[\operatorname{sgn}(y-y_i)-\operatorname{sgn}(y-y_j)] - \frac{2}{6}\sum_i \mathbf{v}_i\cdot\mathbf{F}_i^{(3)} \\ &\times\operatorname{sgn}(y-y_i) + \frac{1}{6}\sum_{ik} \mathbf{v}_i\cdot\mathbf{F}_i^{(3)}\operatorname{sgn}(y-y_k) \\ &+ \frac{1}{6}\sum_{ij} \mathbf{v}_i\cdot\mathbf{F}_i^{(3)}\operatorname{sgn}(y-y_j) + \frac{3}{6}\sum_i \mathbf{u}\cdot\mathbf{F}_i^{(3)} \\ &\times\operatorname{sgn}(y-y_i). \end{aligned} \tag{A2}$$

The-three body potential contribution can be isolated as

$$\begin{aligned} J_{qy}^{U(3)}(y,t) = &-\frac{3}{6A}\sum_i \mathbf{v}_i\cdot\mathbf{F}_i^{(3)}\operatorname{sgn}(y-y_i) \\ &+ \frac{1}{6A}\sum_i \mathbf{v}_i\cdot\mathbf{F}_i^{(3)}\operatorname{sgn}(y-y_i) \\ &+ \frac{1}{6A}\sum_{ik} \mathbf{v}_i\cdot\mathbf{F}_i^{(3)}\operatorname{sgn}(y-y_k) \\ &+ \frac{1}{6A}\sum_{ij} \mathbf{v}_i\cdot\mathbf{F}_i^{(3)}\operatorname{sgn}(y-y_j) \\ &+ \frac{3}{6A}\sum_i \mathbf{u}\cdot\mathbf{F}_i^{(3)}\operatorname{sgn}(y-y_i) \\ = &-\frac{1}{2A}\sum_i [\mathbf{v}_i-\mathbf{u}(y)]\cdot\mathbf{F}_i^{(3)}\operatorname{sgn}(y-y_i) \\ &+ \frac{1}{6A}\sum_{ijk} \mathbf{v}_i\cdot\mathbf{F}_i^{(3)}[\operatorname{sgn}(y-y_i)+\operatorname{sgn}(y-y_j) \\ &+ \operatorname{sgn}(y-y_k)]. \end{aligned} \tag{A3}$$

To prove that Eq. (A3) [i.e., three-body contribution to Eq. (27)] is identical to the three-body contribution of Eq. (26), let us expand Eq. (A3):

$$\begin{aligned} J_{qy}^{U(3)}(y,t) &= -\frac{1}{2A}\sum_i [\mathbf{v}_i-\mathbf{u}(y)]\cdot\mathbf{F}_i^{(3)}\operatorname{sgn}(y-y_i) + \frac{1}{6A}\sum_{ijk} \mathbf{v}_i\cdot\mathbf{F}_i^{(3)}[\operatorname{sgn}(y-y_i)+\operatorname{sgn}(y-y_j)+\operatorname{sgn}(y-y_k)] \\ &= -\frac{1}{2A}\sum_i \mathbf{v}_i\cdot\mathbf{F}_i^{(3)}\operatorname{sgn}(y-y_i) + \frac{1}{2A}\sum_i \mathbf{u}\cdot\mathbf{F}_i^{(3)}\operatorname{sgn}(y-y_i) \\ &\quad + \frac{1}{6A}\sum_{ijk} \mathbf{v}_i\cdot\mathbf{F}_i^{(3)}[\operatorname{sgn}(y-y_i)+\operatorname{sgn}(y-y_j)+\operatorname{sgn}(y-y_k)] \\ &= -\frac{1}{2A}\sum_i \mathbf{v}_i\cdot\mathbf{F}_i^{(3)}\operatorname{sgn}(y-y_i) + \frac{1}{6A}\mathbf{u}\cdot\sum_{ijk}\{\mathbf{F}_i^{(3)}\operatorname{sgn}(y-y_i)+\mathbf{F}_j^{(3)}\operatorname{sgn}(y-y_j)+\mathbf{F}_k^{(3)}\operatorname{sgn}(y-y_k)\} \\ &\quad + \frac{1}{6A}\sum_{ijk} \mathbf{v}_i\cdot\mathbf{F}_i^{(3)}[\operatorname{sgn}(y-y_i)+\operatorname{sgn}(y-y_j)+\operatorname{sgn}(y-y_k)] \\ &= -\frac{3}{6A}\sum_i \mathbf{v}_i\cdot\mathbf{F}_i^{(3)}\operatorname{sgn}(y-y_i) + \frac{1}{6A}\mathbf{u}\cdot\left\{\begin{array}{l} \sum_{ij} \mathbf{F}_{ij}^{(3)}[\operatorname{sgn}(y-y_i)-\operatorname{sgn}(y-y_j)]+ \\ \sum_{ik} \mathbf{F}_{ik}^{(3)}[\operatorname{sgn}(y-y_i)-\operatorname{sgn}(y-y_k)]+ \\ \sum_{jk} \mathbf{F}_{jk}^{(3)}[\operatorname{sgn}(y-y_j)-\operatorname{sgn}(y-y_k)] \end{array}\right\} \end{aligned}$$

$$+\frac{1}{6A}\sum_{ijk}\mathbf{v}_i\cdot(\mathbf{F}_{ij}^{(3)}+\mathbf{F}_{ik}^{(3)})\mathrm{sgn}(y-y_i)+\frac{1}{6A}\sum_{ijk}\mathbf{v}_i\cdot(\mathbf{F}_{ij}^{(3)}+\mathbf{F}_{ik}^{(3)})$$

$$\times\mathrm{sgn}(y-y_j)+\frac{1}{6A}\sum_{ijk}\mathbf{v}_i\cdot(\mathbf{F}_{ij}^{(3)}+\mathbf{F}_{ik}^{(3)})\mathrm{sgn}(y-y_k)$$

$$=-\frac{1}{6A}\sum_{ij}[\mathbf{v}_i-\mathbf{u}(y)]\cdot\mathbf{F}_{ij}^{(3)}[\mathrm{sgn}(y-y_i)-\mathrm{sgn}(y-y_j)]-\frac{1}{6A}\sum_{ik}[\mathbf{v}_i-\mathbf{u}(y)]\cdot\mathbf{F}_{ik}^{(3)}[\mathrm{sgn}(y-y_i)-\mathrm{sgn}(y$$

$$-y_k)]-\frac{1}{6A}\sum_{ijk}\mathbf{v}_i\cdot\mathbf{F}_{ij}^{(3)}[\mathrm{sgn}(y-y_i)-\mathrm{sgn}(y-y_k)]-\frac{1}{6A}\sum_{ijk}\mathbf{v}_i\cdot\mathbf{F}_{ik}^{(3)}[\mathrm{sgn}(y-y_i)-\mathrm{sgn}(y-y_j)]$$

$$+\frac{1}{6A}\sum_{jk}\mathbf{u}(y)\cdot\mathbf{F}_{jk}^{(3)}[\mathrm{sgn}(y-y_j)-\mathrm{sgn}(y-y_k)]. \tag{A4}$$

Equation (A4) is just the three-body contribution to Eq. (26), as required.

[1] M. Kroger and S. Hess, Phys. Rev. Lett. **85**, 1128 (2000).
[2] J. D. Moore, S. T. Cui, P. T. Cummings, and H. D. Cochran, AIChE J. **43**, 3260 (1997).
[3] S. Bair, C. McCabe, and P. T. Cummings, Phys. Rev. Lett. **88**, 058302-1 (2002).
[4] P. J. Daivis, M. L. Matin, and B. D. Todd, J. Non-Newtonian Fluid Mech. **111**, 1 (2003).
[5] L. I. Kioupis and E. J. Maginn, J. Phys. Chem. B **103**, 10 781 (1999).
[6] K. P. Travis and K. E. Gubbins, J. Chem. Phys. **112**, 1984 (2000).
[7] S. T. Cui, C. McCabe, P. T. Cummings, and H. D. Cochran, J. Chem. Phys. **119**, 8941 (2003).
[8] F. Varnik and K. Binder, J. Chem. Phys. **117**, 6336 (2002).
[9] J. Delhommelle and D. J. Evans, Mol. Phys. **100**, 2857 (2002).
[10] X. J. Fan, N. Phan-Thien, N. T. Yong, and X. Diao, Phys. Fluids **14**, 1146 (2002).
[11] S. Y. Liem, D. Brown, and J. H. R. Clarke, Phys. Rev. A **45**, 3706 (1992).
[12] J. H. Irving and J. G. Kirkwood, J. Chem. Phys. **18**, 817 (1950).
[13] B. D. Todd, D. J. Evans, and P. J. Daivis, Phys. Rev. E **52**, 1627 (1995).
[14] B. D. Todd, P. J. Daivis, and D. J. Evans, Phys. Rev. E **51**, 4362 (1995).
[15] D. R. J. Monaghan and G. P. Morriss, Phys. Rev. E **56**, 476 (1997).
[16] P. J. Daivis, K. P. Travis, and B. D. Todd, J. Chem. Phys. **104**, 9651 (1996).
[17] A. Baranyai, Phys. Rev. E **54**, 6911 (1996).
[18] T. Ikeshoji, B. Hafskjold, and H. Furuholt, Mol. Simul. **29**, 101 (2003).
[19] B. Hafskjold and H. Furuholt, Phys. Rev. E **66**, 011203 (2002).
[20] S. T. Cui, P. T. Cummings, and H. D. Cochran, J. Chem. Phys. **114**, 7189 (2001).
[21] F. Varnik, J. Baschnagel, and K. Binder, J. Chem. Phys. **113**, 4444 (2000).
[22] K. Van Workum and J. J. de Pablo, Phys. Rev. E **67**, 031601 (2003).
[23] O. G. Jepps and S. K. Bhatia, Phys. Rev. E **67**, 041206 (2003).
[24] J. A. Barker, R. A. Fisher, and R. O. Watts, Mol. Phys. **21**, 657 (1971).
[25] B. M. Axilrod and E. Teller, J. Chem. Phys. **11**, 299 (1943).
[26] G. Marcelli, B. D. Todd, and R. J. Sadus, Phys. Rev. E **63**, 021204 (2001).
[27] S. H. Lee and P. T. Cummings, J. Chem. Phys. **99**, 3919 (1993); **101**, 6206 (1994).
[28] J. A. Barker and A. Pompe, Aust. J. Chem. **21**, 1683 (1968).
[29] M. V. Bobetic and J. A. Barker, Phys. Rev. B **2**, 4169 (1970).
[30] P. J. Leondard and J. A. Barker, in *Theoretical Chemistry: Advances and Perspectives*, edited by H. Eyring and D. Henderson (Academic, London, 1975) Vol. 1.
[31] G. Marcelli and R. J. Sadus, J. Chem. Phys. **111**, 1533 (1999).
[32] K. P. Travis, B. D. Todd, and D. J. Evans, Phys. Rev. E **55**, 4288 (1997).